Available online at www.sciencedirect.com
SCIENCE DIRECT®
Journal of Power Sources 134 (2004) 49–56
JOURNAL OF POWER SOURCES
www.elsevier.com/locate/jpowsour

Analysis of a heat recirculating cooler for fuel gas sulfur removal in solid oxide fuel cells

Geo. A. Richards [a,*], David A. Berry [a], Adam Freed [b]

[a] National Energy Technology Laboratory, US Department of Energy, Morgantown, WV 26505, USA
[b] REM Engineering Services, PLLC, 3537 Collins Ferry Road, Morgantown, WV 26505, USA

Received 5 February 2004; accepted 1 March 2004

Abstract

When using conventional fossil fuels, most fuel cell systems require sulfur removal as part of their fuel processing. A novel approach to enable conventional sulfur removal in high-temperature fuel processing is presented. Using established principles from heat-recirculating combustors, it is suggested that high-temperature syngas can be momentarily cooled to conditions that would permit conventional sulfur removal to be carried out at relatively low temperatures. The recirculated heat is then used to heat the gas back to conditions that are minimally less than the original temperature. A model for evaluating the performance of this concept is presented, and calculations suggest that relative to fuel cell applications, reasonable physical dimensions can be expected in actual applications. For high-pressure syngas (i.e., coal gasification), the physical dimensions will rise with the operating pressure.

Keywords: Heat recirculation; Sulfur removal; Fuel gas; Fuel processing; Fuel cell; Reforming

1. Introduction

Fuel processing is an essential component of fuel cell systems that use conventional hydrocarbons. Compared to other types of fuel cells, the higher operating temperature of solid oxide fuel cells offers advantages for fuel processing. Early generation tubular SOFCs operate near 1000 °C [1] while advanced planar designs being developed in the Department of Energy's Solid State Energy Conversion Alliance (SECA) may operate at 800 °C, or lower [2]. Within this temperature range, heat from the fuel cell exhaust can be readily used to reform hydrocarbons to syngas ideally containing hydrogen and carbon monoxide. The carbon monoxide can be readily used by the SOFC anode, and also in molten carbonate fuel cells. This avoids complex CO shift reactors which are otherwise needed, for example, in PEM fuel cell systems. However, none of the fuel cell systems can tolerate appreciable quantities of sulfur in the fuel gas. In the future, it is anticipated that improved sulfur tolerance in SOFC anodes, along with continued reduction in fuel sulfur content will allow fuel cells to operate without any sulfur removal. However, at the present time, sulfur removal is required for cell operation, and will continue to be required where high-sulfur fuel is available. There are two broad approaches to deal with sulfur in the hydrocarbon fuel supply: remove it before reforming the fuel, or remove it from the syngas after reforming. Both approaches have their limitations. If the sulfur is removed before conversion to syngas, the sulfur removal must be successful on any sulfur form that is present in the feedstock. Given the variety of organic sulfur compounds found, for example, in heavy distillate fuels, hydrotreatment is proposed as a method to convert the sulfur species to H_2S, then remove the H_2S prior to reforming. In contrast, if sulfur is removed after reforming, the sulfur will already be found as hydrogen sulfide. Techniques to remove hydrogen sulfide are well-established for some temperature ranges. For example, zinc-oxide absorbents are very effective at capturing sulfur at temperature below 400 °C [3]. More recently Gardner et al. [4] have shown that catalytic oxidation of H_2S can capture sulfur at temperatures below 200 °C. These temperatures are lower than the fuel cell or fuel processor operating temperature, and thus present a dilemma for thermal integration: temperatures that are ideally suited for fuel processing and fuel cell operation are higher than the temperatures needed to utilize existing sulfur removal technologies. This issue is shown schematically in Fig. 1. A conceptual solid

* Corresponding author. Tel.: +1-304-285-4458; fax: +1-304-285-4403.
E-mail address: george.richards@netl.doe.gov (G.A. Richards).

0378-7753/$ – see front matter © 2004 Elsevier B.V. All rights reserved.
doi:10.1016/j.jpowsour.2004.03.030

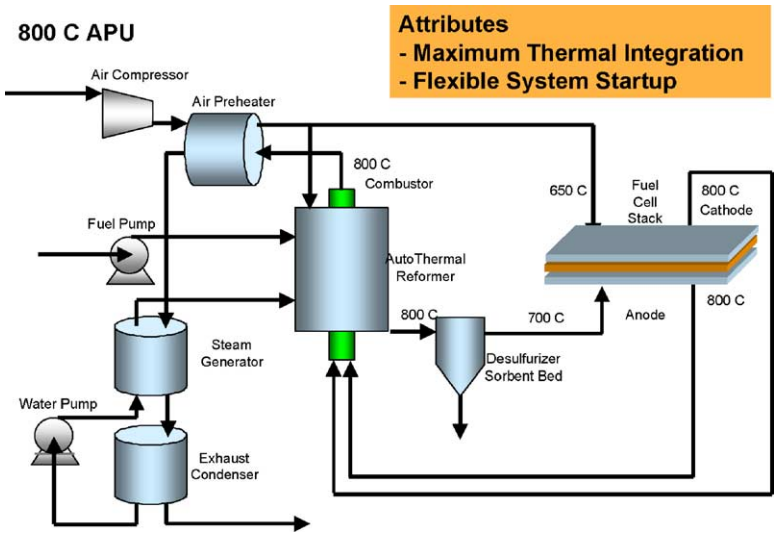

Fig. 1. Conceptual fuel cell system, using thermal integration and high temperature sulfur removal.

oxide fuel cell system is shown which uses the exhaust heat from the solid oxide fuel cell at 800 °C to reform the fuel. By integrating the heat with the fuel processor, total system efficiencies including fuel processing from conventional hydrocarbons have been calculated to approach 50% [5]. However, the sulfur removal step shown in the Fig. 1 is conceptual. At these temperatures, there are currently no methods to remove H_2S from syngas to desired levels ($<\sim$1 ppmv) without rejecting appreciable quantities of thermal energy. A simple method to lower the gas temperature to enable conventional sulfur removal is needed, yet without rejecting significant quantities of heat. In essence, the goal is to drop the temperature, remove the sulfur, and then heat the gas back up while losing as little thermal energy as possible.

This paper explores the performance of a heat recirculating concept that can produce gas temperature reductions that may enable sulfur removal at overall relatively high temperatures. The concept borrows from established technology in heat-recirculating burners. In heat recirculating burners, the goal is to increase the gas temperature, burn the reactants, and then cool the gas with as little heat input as possible to maintain combustion. As will be shown, the heat recirculating burner is essentially the opposite thermal problem as what is proposed here. For this reason, a brief review of the concept of heat-recirculating combustion is presented next.

2. Review of heat recirculating combustion

The concept of using heat recirculation in combustion has been used in various forms for many years. Lloyd and Weinberg [6,7] presented the first description of how heat recirculation, without mixing products and reactants, could be used to burn mixtures which have very low heating values. The process is shown conceptually in Fig. 2. The graph at the top shows the temperature of the reactants as the gases move

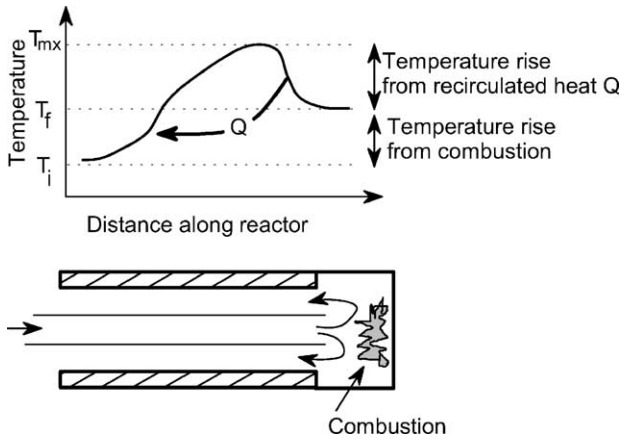

Fig. 2. Temperature history of gas in a heat recirculating burner.

along the flow path of the reactor. Reactants at initial temperature T_i enter at the left in a central tube which is heated by combustion products exiting in a co-annular duct. These gases are progressively heated until they enter the combustion chamber at the right, where heat is released.[1] The gas temperature raises due to heat release to a maximum temperature T_{max}, and then exit the reactor flowing right to left. The products are progressively cooled as they flow down the annulus and provide the recirculated heat Q to the incoming reactants. The gases exit at the final temperature T_f which is determined entirely by the heat provided by combustion.

Lloyd and Weinberg [6,7] pointed out that the maximum temperature T_{max} is determined by the amount of heat recirculated Q, producing temperatures which are "super-adiabatic", i.e., higher than would be achieved in adiabatic combustion without heat recirculation. Ignoring

[1] Fuel and oxidant may be kept separate until this point, but this is not shown for simplicity.

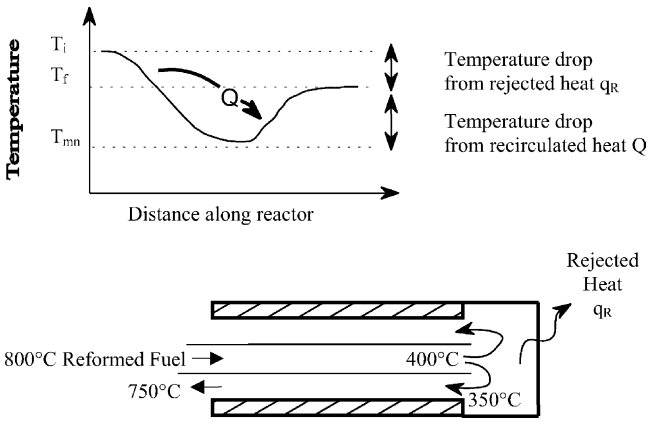

Fig. 3. Heat recirculation concept to produce low temperatures.

dissociation, and material limits, very high temperatures can be achieved with very small heat input. This will allow combustion to proceed in gases which might otherwise not produce enough temperature rise to sustain combustion. These ideas were reviewed by Weinberg [8,9] and have spawned various commercial applications, see for example the discussion of thermal oxidizers by Baukal [10]. Using heat recirculation to produce super-adiabatic flame temperatures has led to the development of the so-called high-temperature air combustion. This technology has demonstrated remarkable improvements in thermal efficiency of process heaters, with surprisingly good emissions performance—see the recent monogram by Tsuji et al. [11]. Drayton et al. [12] used the super-adiabatic temperatures produced by heat recirculation in a novel method to reform hydrocarbons to syngas. This concept may be of interest as an alternative to catalytic, partial oxidation, or steam fuel reforming.

Thus, there have been numerous technical applications using heat recirculation to produce temperatures which are higher than possible from direct heat addition (usually via combustion). However, to the authors' knowledge, there have been no investigations of the reverse problem: using heat recirculation to produce temperatures which are lower than possible from direct heat rejection. The concept is shown in Fig. 3. Fluid at initial temperature T_i enters at the left in a central tube which is cooled by the fluid exiting right to left in the co-annular duct. Fluid in the central tube is progressively cooled until it enters the chamber at the right, where heat is rejected at rate q_R. The temperature of the fluid drops due to heat rejection to the atmosphere, using cooling fins, etc. This produces the minimum temperature T_{min} in the flow path, and would be the point where, for example, sulfur removal could be carried out. The cooled fluid exits the reactor flowing right to left via the outer annulus. The fluid is progressively heated as it flows down the annulus and absorbs the recirculated heat Q from the incoming fluid. The fluid exits at the final temperature T_f which is determined entirely by the heat rejected. Fig. 3 shows example temperatures for the case where the heat recirculating cooler is located downstream from a fuel reforming device. The reformed fuel enters at 800 °C and is cooled to 400 °C as it flows through the inner annulas. Heat is then rejected, which further reduces the temperature to 350 °C. At this point, sulfur removal is preformed and as the fuel exits, it is reheated from 350 to 750 °C.

For practical application of the proposed concept to fuel cell systems, the question is posed: for reasonable design parameters, can a minimum temperature T_{min} be achieved that will permit conventional sulfur removal techniques to be used? The analysis used to answer this question is presented next. The design parameters include the physical size of the heat recirculating system, and the permissible heat rejection (i.e., the temperature drop $T_i - T_f$, Fig. 3).

3. Analysis of the heat recirculating cooler

The nomenclature is shown in Fig. 4. At the right side of Fig. 4, a proposed arrangement using stacked heat transfer elements is shown for later reference. At the left side, the nomenclature for a single element is shown. Note that the adiabatic walls of the single element are used as a convenience; these would correspond to the centerline of the symmetric channel flow in the stacked arrangement. The end stations of the flow channels are identified with the indices 1 and 2, and the length L of both flow channels. The subscripts 'c' and 'h' are used to distinguish fluid in the "hot" or "cold" channel. The input mass flow m_h enters at temperature T_{h1} and velocity V_{h1}. The flow travels along a channel having height H as shown, with a width W into the plane of the figure. Heat is transferred from the hot channel flow to the cold channel flow across a thin sheet. The external

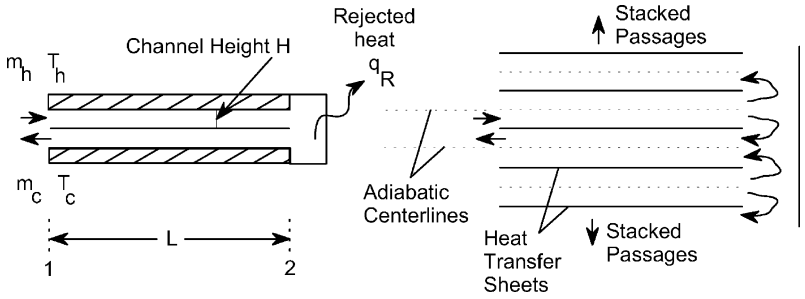

Fig. 4. Nomenclature of heat recirculation cooler analysis.

walls of both the hot and cold channels are treated as adiabatic surfaces. The flow enters a chamber situated at the exit of the hot channel flow, where heat is rejected at rate q_R by a cooling fin, cooling system, etc. The flow then turns backward and proceeds through the cold channel where heat is absorbed from the hot channel flow. Flow exits the cold channel at temperature T_{c1}. In the arrangement shown, no mass is added or lost, so that the exit mass flow equals the input mass flow, $m_c = m_h$. These equal quantities are distinguished for the purposes of a more general analysis where mass may be added or subtracted.

The analysis is essentially the same as that found in standard textbooks treating counter flow heat exchangers; see for example Incropera and DeWitt [13]. A notable issue for this analysis is that the same fluid is circulated on both sides of the heat transfer membrane. This introduces some changes compared to what is often presented in heat exchanger design where the fluids are usually different.

For the purposes of analysis, a differential element from the flow channels is considered in Fig. 5. The heat transfer sheet is sandwiched between coordinate systems x_h and x_c which are aligned with the flow in the hot and cold channels, respectively. The differential element is length dx_c, or dx_h in the respective coordinate systems. At steady state, the heat flow per unit area q'' is the same on both sides of the sheet; storage in the sheet is ignored. Performing a differential energy balance on the fluid in both the hot and cold channels leads to the following expressions:

$$m_h C_{ph}\, dT_h = -q'' W\, dx_h \tag{1}$$

$$m_c C_{pc}\, dT_c = q'' W\, dx_c \tag{2}$$

These equations simply state that the enthalpy rise in the cold channel is matched by the enthalpy reduction in the hot channel. Note that $x_c = L - x_h$ so that $dx_c = -dx_h$ and consider the case where the mass flow and specific heat of both the hot and cold fluids are the same, designated as mC_p. In this situation, the resulting temperature slopes are as follows:

$$\frac{dT_h}{dx_h} = \frac{-q'' W}{mC_p} \tag{3}$$

$$\frac{dT_c}{dx_h} = \frac{-q'' W}{mC_p} \tag{4}$$

Thus, viewed in the x_h coordinates, both temperatures have the same slope. Taking the difference of Eqs. (3) and (4) shows that the difference between the hot and cold temperature must be constant along the length of the device:

$$\frac{d(T_h - T_c)}{dx_h} = 0, \quad T_h - T_c = \text{constant} \tag{5}$$

The heat transfer per unit area q'' is calculated from the overall heat transfer coefficient U and the local temperature difference:

$$q'' = U(T_h - T_c) \tag{6}$$

Although Eq. (5) shows that the temperature difference is constant along the flow axis, the overall heat transfer coefficient U changes with the gas temperatures so that the heat transfer varies modestly along the flow axis. Thus, a plot of the temperature profile is shown in Fig. 6. The slope of both temperature curves is determined entirely from the heat transfer term on the right side of Eq. (3) or (4), but the difference in temperature remains constant along the axis of the device. The difference in temperature between the hot and cold streams is found from an overall energy balance:

$$T_{h1} - T_{c1} = \frac{q_R}{mC_p}, \qquad T_{h2} - T_{c2} = \frac{q_R}{mC_p} \tag{7}$$

Combining Eq. (6) with the slopes of the temperature gradients calculated from Eq. (3) or (4) results in:

$$\frac{dT_h}{dx_h} = \frac{dT_c}{dx_h} = \frac{-U\Delta T W}{mC_p} \tag{8}$$

It is more convenient to express the mass flow in terms of a bulk velocity V in the channel. The velocity will be greatest at the entrance to the hot channel, so that the velocity used for reference will refer to the hot channel, station 1 (subscript

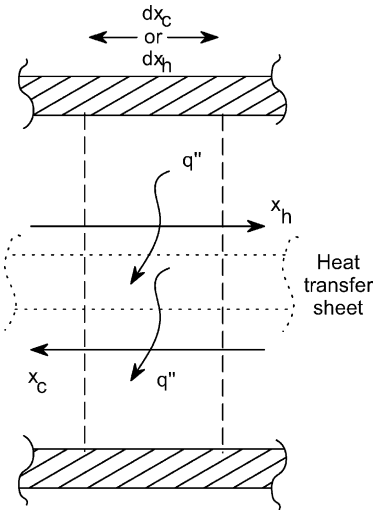

Fig. 5. Differential element for heat balance.

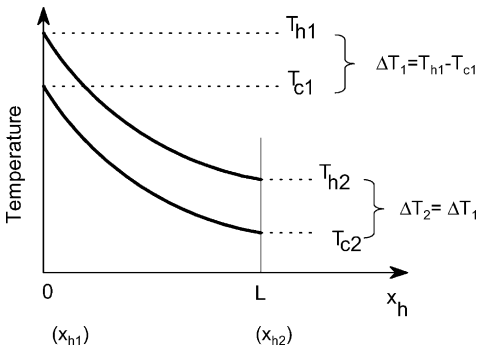

Fig. 6. Sketch of temperature profiles along the axis of the device.

h1). Expressing the mass flow as the product of density ρ_{h1}, velocity V_{h1} and channel area (WH = channel area):

$$\frac{dT_h}{dx_h} = \frac{dT_c}{dx_h} = \frac{-U\Delta T}{\rho_{h1} V_{h1} H C_p} \quad (9)$$

Thus, the slope of the temperature can be calculated for the parameters on the right side of Eq. (9). To achieve the shortest practical design for a temperature reduction, it is desirable to maximize the magnitude of the slope. The slope is largest for low velocities and high heat transfer coefficient U. To consider specific examples, it is necessary to calculate the overall heat transfer coefficient U. From standard textbooks on heat transfer [13], this is:

$$U = \frac{1}{1/h_c + t_s/k_s + t/h_h} \quad (10)$$

The subscript 's' denotes the steel separating sheet between the hot and cold channels, t_s is the thickness, k_s is the thermal conductivity of the steel, and the h_c and h_h are the respective cold and hot convection coefficients. Because the temperature difference across the sheet is (by intent) relatively small, the transport properties can be calculated from either the hot or cold side conditions at any station x with little error; the hot temperature is used in calculations below. For turbulent flow, the convection coefficients will rise with the Reynolds number to a fractional power, so increasing the flow velocity will increase the heat transfer coefficient until the conduction across the sheet becomes a limiting factor. In contrast, for laminar flow in the channels, the convection coefficients are independent of the flow rate. Noting the velocity in Eq. (9), the implication is that the greatest slopes can be achieved by using the smallest practical velocity in Eq. (9). For this reason, calculations are carried out for relatively small flow velocities, typical of the range of velocities found in fuel cell flow passages.

The convection coefficient is calculated from the standard Nusselt number for laminar flow inside a channel with constant heat flux (see [13]). Gaseous mixtures are of most interest, requiring calculation of the mixture properties, rather than just single species. Thermodynamic and transport properties of species in the mixture were taken from [13–15]. Mixture thermodynamic properties (ρ and C_p) were calculated from ideal gas mixing. This mixture thermal conductivity is calculated using the approach found in [16]. The metal sheet which divides the flow channel was assumed to be a 0.79 mm thick sheet of type 304 stainless. For the conditions studied here, the resistance to heat transfer across the flow channels was dominated by the convection coefficients, not the dividing metal sheet. It is important to note that a practical embodiment of this concept may include channels stacked one on top of another, as shown in Fig. 4. In this situation, the adiabatic boundary shown in Fig. 4 would correspond to the mid-plan of a channel. In other words, the physical distance to the next metal sheet would be $2H$, not H.

Eq. (9) must be integrated over a desired temperature range to determine the needed length of a heat-exchanger. It is significant to recognize that the transport and thermodynamic properties of the gases of interest vary appreciably with temperature. Gas and stainless steel properties were calculated over the range of temperatures, and used to integrate (9) to determine the heat exchanger length needed to produce a desired minimum temperature. The results are described next.

4. Results

To make the calculations relevant to reforming of heavy hydrocarbons, an input fuel is approximated as $CH_{1.75}$. Gas compositions of ideal steam reforming and ideal partial oxidation (POX) with air are considered with the following stoichiometries:

- Ideal steam reforming: $CH_{1.75} + H_2O \rightarrow 1.875H_2 + CO_2$.
- Ideal POX with air: $CH_{1.75} + (1/2)(O_2 + 3.76N_2) \rightarrow 0.88H_2 + CO + 1.88N_2$.

In addition to the gas compositions produced by the reforming processes above, calculations have been carried out for pure hydrogen, pure steam, and air. Comparing results for these various gas compositions will demonstrate the range of behaviors that are expected in different applications. The various gas compositions and other parameters are summarized in Table 1. As noted above, the flow velocity at the hot entrance is chosen to yield a reasonable device length.

Using the above parameters, the temperature slope was calculated over a range of temperatures from 300 to 1200 °C. The results are shown in Fig. 7. These temperature slopes can be used to quickly compare the length L that is needed for heat exchange among the various gases simply by approximating $dT/dx \sim (T_{h1} - T_{h2})/L$. Because of the very large thermal conductivity of hydrogen, and low density, the temperature slope is very large. The implication is that a very compact heat exchanger (small value of L) can be used where the fuel is largely composed of hydrogen. At the other extreme, the modest thermal conductivity of air or

Table 1
List of gas compositions and other parameters

	H_2	CO	H_2O	N_2	CO_2	Air
Ideal steam reforming	0.65	0	0	0	0.35	0
Ideal POX reforming with air	0.23	0.27	0	0.5	0	0
Pure hydrogen	1	0	0	0	0	0
Air	0	0	0	0	0	1
Steam	0	0	1	0	0	0

Reforming cases correspond to $CH_{1.75}$—hot inlet velocity, V_{h1}: 2.5 m/s (range from 2.0 to 22.4 m/s); operating pressure: 101 kPa; channel height, H: 1 mm (note comments on stacked geometry); sheet thickness, t_s: 0.79 mm, 304 stainless steel; temperature drop: 25–50 °C (ΔT_2).

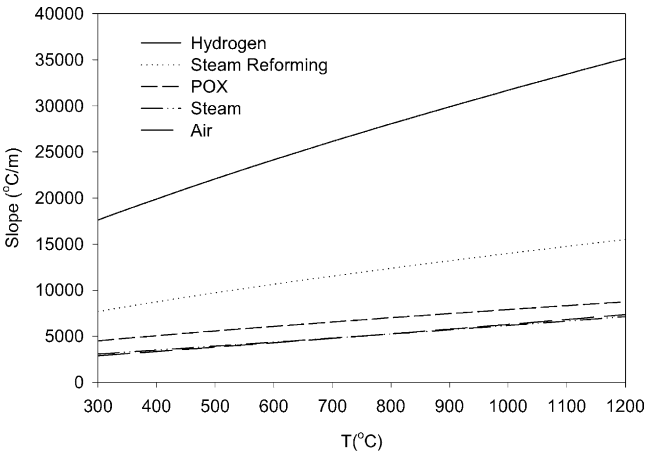

Fig. 7. Temperature slopes for various gases over a range of temperatures. Input parameters are listed in Table 1.

steam produces a relatively smaller temperature slope, indicating that fuels diluted with air and steam would require a longer heat exchanger. It is also instructive to note that the slope drops with temperature due to the declining thermal conductivity of all the gases with temperature, as well as the increasing density in the denominator of Eq. (9).

This equation can be directly integrated to report the length L needed for a given temperature reduction. And the inverse can also be done; if the length is chosen, then the amount of heat rejected can be determined for a given set of conditions. Again using the parameters in Table 1, the heat exchanger length for a temperature reduction down to 600, 400 and 200 °C were calculated for the various gas mixtures. The results are shown in Fig. 8. For the choice of parameters given here, the lengths L are reasonable, and would compare to the dimensions of fuel cell systems that are currently being developed. Comparing the lengths required for the three different temperature drop cases, the relationship between the length L and the temperature drop is almost linear.

To investigate the choice of different operating parameters, a heat exchange length of 0.154 m (6 in.) was selected as a reasonable length for the device. The inlet velocity V_{h1} required to produce the desired minimum temperature was calculated (velocity changes along the length due to temperature variation were incorporated in the calculations). The velocity to achieve temperature change in the hot stream of 800–400 °C was determined for different gas compositions. In Fig. 9, results are shown for $\Delta T_2 = 50\,^{\circ}\mathrm{C}$ and a more efficient case of $\Delta T_2 = 25\,^{\circ}\mathrm{C}$; i.e., with less heat rejection. The highest throughput is possible with hydrogen, using the greater value of heat rejection, $\Delta T_2 = 50\,^{\circ}\mathrm{C}$. At this condition, the viscous pressure drop for the hydrogen flow in the passages was calculated at 290 Pa, which is very small, and could be supplied by a simple fan. If even lower pressure drop were desired to drive the flow, reduced throughput, with corresponding less heat rejection could be used. As shown in the figure, rejecting half as much heat ($\Delta T_2 = 25\,^{\circ}\mathrm{C}$ versus 50 °C), requires reducing the throughput by a factor of 2. Thus, for a given gas composition, design parameters such as throughput and heat rejection can be traded to meet the requirements of pressure drop and device size.

In one final analysis, the amount of rejected heat (indicated by ΔT_2) was calculated for various cases where the heat exchange length and gas velocity were held constant. Results are shown in Fig. 10 where the hot gas initial temperature is $T_{h1} = 800\,^{\circ}\mathrm{C}$. For gases composed primarily of air or steam, achieving a minimum temperature of 200 °C requires $\Delta T_2 = 55\,^{\circ}\mathrm{C}$. This temperature drop represents approximately 4.6% of the enthalpy in the initial hot stream. As already noted, this amount of heat rejection can be reduced by choosing a lower value of V_{h1}, or by making the device longer. Because of the thermal properties of hydrogen, the heat rejection for the same operating conditions is

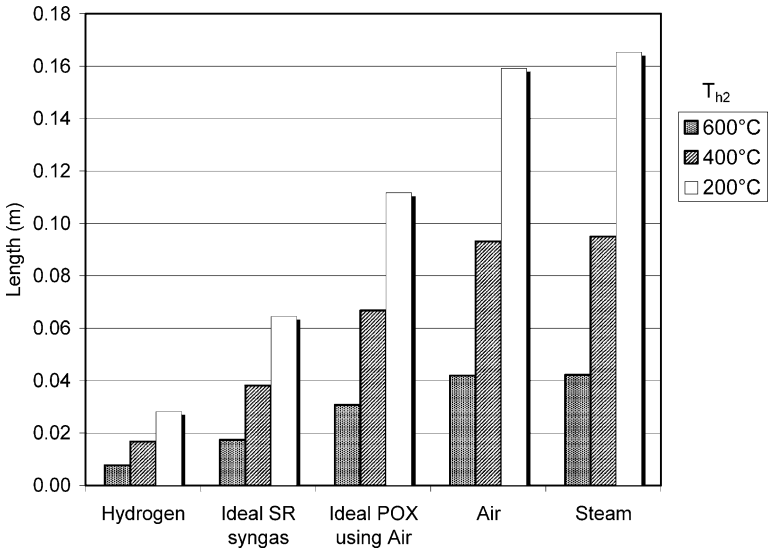

Fig. 8. Calculated heat exchanger length for different gases, and temperature drops. $\Delta T_2 = 50\,^{\circ}\mathrm{C}$, $V_{h1} = 2.5$ m/s.

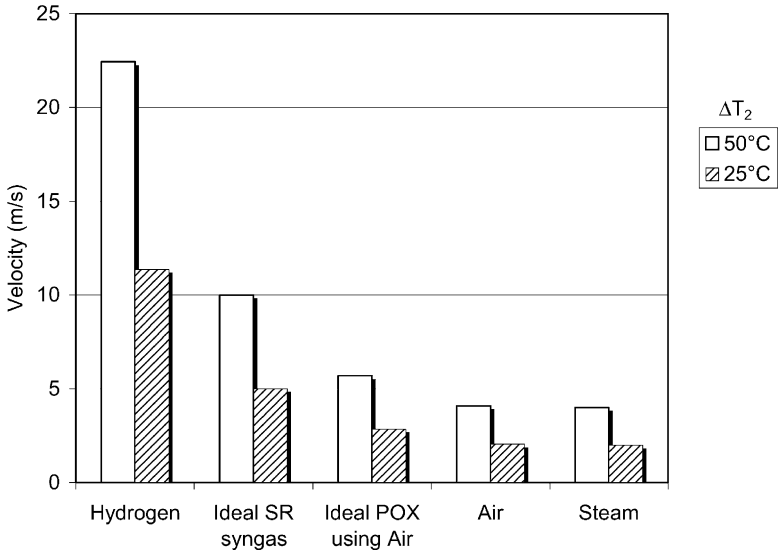

Fig. 9. Calculated inlet gas velocity for different gases and rejected temperature drops. The heat exchanger length is constant at 0.154 m (6 in.) and the hot stream conditions are $T_{h1} = 800\,^{\circ}C$, $T_{h2} = 400\,^{\circ}C$.

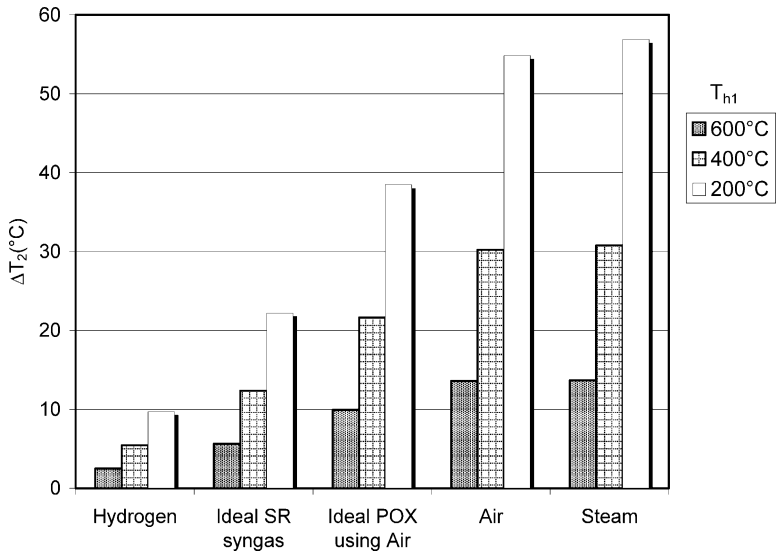

Fig. 10. Required temperature drop for different gases and temperature drop. A 0.154 m (6 in.) heat exchange length is used in all the cases. The inlet gas velocity, V_{h1}, is constant at 2.5 m/s and the inlet gas temperature is $T_{h1} = 800\,^{\circ}C$.

50–80% less compared to the other gases. Under the least severe condition of $T_{h2} = 600\,^{\circ}C$, there only needs to be $2.5\,^{\circ}C$ of temperature difference between the streams. In practice, this small temperature difference would be difficult to control, and the heat rejection could be increased while allowing a higher throughput.

It is useful to consider if or how this concept could be used in larger systems such as coal gasifiers, which may operate at high gas pressures in excess of 30 atm. While there is nothing preventing such an application, it should be noted that higher operating pressure increases the gas density. Referring to Eq. (9), the higher gas density produces a corresponding reduction in temperature slope, meaning that device will be longer for the same operating conditions, i.e., scaling approximately with the gas pressure. Given the lengths calculated for atmospheric pressure (Fig. 8), even a 30-fold increase would be a reasonable size heat exchanger for large gasifier applications. The specific tradeoffs are the subject of ongoing evaluation.

5. Summary and conclusions

Because most fuel cell systems cannot tolerate sulfur, it is necessary to remove the sulfur from syngas generated from reforming or gasifying heavy fuels. Existing techniques to remove sulfur are not thermally matched to the fuel processor or fuel cell system temperatures, and would require

significant heat rejection and loss of efficiency to remove the sulfur. The results presented above demonstrate that it is possible to use heat recirculation as a method to lower the temperature of syngas, reject a small amount of heat, and then raise the temperature to a value slightly lower than the original flow. This is essentially the inverse of the principle that is used in low-heat content fuel burners. In these burners, recirculated heat is used to increase the reactant temperature, release a small amount of chemical energy, and then lower the temperature of the combustion products to a value slightly higher than the original flow.

Calculations presented here are used to evaluate the physical dimensions of a heat-recirculating device needed to produce temperatures suitable for sulfur removal (200–400 °C). Using flow velocities typical of the channels of fuel cell passages, and accepting a heat loss of 50 °C (or less) from an initial temperature of 800 °C, the required physical length of the heat exchanger passage to produce a 400 °C condition ranges from 2 to 20 cm, depending on the composition of the gases involved. It should be noted that Eq. (9) can be used to estimate the effect of choosing different parameters. Choosing to reject less energy (ΔT_2) or increase the inlet velocity V_{h1} would decrease the temperature slope and lengthen the device.

References

[1] J.H. Hirschenhofer, D.B. Stauffer, R.R. Engleman, Fuel Cells Handbook, DOE/METC-94/1006 (E94004072), Available at National Technical Information Service, Springfield, VA, 1994.
[2] Proceedings of the Solid State Energy Conversion Alliance Workshop (SECA), Baltimore, MD, Available at National Technical Information Service, Springfield, VA, 1–2 June 2000.
[3] M.V. Twigg (Ed.), Catalyst Handbook, Wolfe Publishing Ltd., 1989.
[4] T.H. Gardner, D.A. Berry, K.D. Lyons, S.K. Beer, A.D. Freed, Fuel 81 (2002) 2157–2166.
[5] D.A. Berry, T.H. Gardner, R.E. James, W. Rogers, D. Shekhawat, Fuel processing of diesel for fuel cells, Annual Report Fuel Cells for Transportation Program, Department of Energy Office of Transportation Technology, November 2002.
[6] S.A. Lloyd, F.J. Weinberg, Nature 251 (1974) 47–49.
[7] S.A. Lloyd, F.J. Weinberg, Nature 257 (1975) 367–370.
[8] F.J. Weinberg, Combustion in heat-recirculating burners, in: F.J. Weinberg (Ed.), Advanced Combustion Methods, Academic Press, 1986, pp. 183–236.
[9] F.J. Weinberg, Combust. Sci. Technol. 121 (1996) 3–22.
[10] C.E. Baukal (Ed.), The John Zinc Combustion Handbook, CRC Press, 2001.
[11] H. Tsuji, A.K. Gupta, T. Hasegawa, M. Katsuki, K. Kishimoto, M. Morita, High-Temperature Air Combustion, CRC Press, 2002.
[12] M.K. Drayton, A.V. Saveliev, L.A. Kennedy, A.A. Fridman, Y. Li, Syngas production using superadiabatic combustion of ultra-rich methane–air mixtures, in: Proceedings of the 27th Symposium (International) on Combustion, The Combustion Institute, Pittsburgh, PA, 1998, pp. 1361–1367.
[13] F.P. Incropera, D.P. DeWitt, Fundamentals of Heat Transfer, Wiley, 1981.
[14] R.H. Perry, D.W. Green, J.O. Maloney, Perry's Chemical Engineers' Handbook, 6th ed., McGraw-Hill, 1984.
[15] R.A. Svehla, Estimated Viscosities and Thermal Conductivities of Gases at High Temperatures, NASA TR R-132, 1962.
[16] R.B. Bird, W.E. Stewart, E.N. Lightfoot, Transport Phenomenon, 2nd ed., Wiley, New York, 2002.